

Optimization of a Tuned Mass Damper Location for Enhanced Chatter Suppression in Thin-Wall Milling

Mohanraj Selvakumar* – Prabhu Raja Venugopal – Gautham Velayudhan
PSG College of Technology, Department of Mechanical Engineering, India

In this paper, a method of optimizing the location of a tuned mass damper (TMD) for enhancing the chatter stability limits of a thin-walled workpiece by using numerical techniques is proposed with due consideration of the mass effect of TMD. The dominant mode of the workpiece is identified from the simulated and measured frequency response functions of the workpiece. Two TMDs each having a single degree of freedom are designed, and a finite element model to predict the response of the workpiece-damper system is developed. The effect of damper location on the chatter stability of the thin-walled workpiece is investigated. Furthermore, the locations for TMDs are optimized for enhanced chatter stability of the workpiece by using response surface methodology. Milling tests were performed on workpieces with and without TMDs. A three-fold improvement in the minimum stable depth of cut is realized after incorporating the TMDs at their optimal locations on the thin-walled workpiece.

Keywords: chatter, thin-wall milling, tuned mass damper, response surface optimization

Highlights

- The dynamics of a thin-wall workpiece is studied using numerical and experimental methods.
- A single degree of freedom tuned mass damper is designed to suppress the dominant mode of the workpiece.
- A numerical model is developed to investigate the effect of the location of the tuned mass damper on the chatter stability of the workpiece.
- The location of the tuned mass damper is optimized to enhance the chatter stability of the workpiece by adopting the response surface method.
- The milling test revealed a three-fold improvement in the critical depth of cut of the workpiece by introducing TMD.

0 INTRODUCTION

Regenerative chatter is a sort of self-excited vibration that occurs during milling and other machining processes. Chatter has several drawbacks, including poor surface finish, shorter tool life, reduced material removal rate, and increased machining noise. Chatter is usually caused by the most compliant element of the structural dynamic chain. Because workpiece is the most compliant part in thin-wall milling, investigations on the chatter stability of the thin-walled part are gaining momentum. Typical thin-walled parts used in aerospace structures are shown in Fig. 1.

Altintas et al. [1] proposed a frequency domain analytical solution for a dynamic milling model based on the zero-order approximation (ZOA) method to predict chatter stability. Budak et al. [2] proposed an analytical method for modelling varying workpiece dynamics and their effect on process stability.

Iglesias et al. [3] stated that stability lobe diagrams (SLDs) aid in the practical selection of the optimum cutting conditions determined either by time domain or frequency domain-based methods. Heng et al. [4] suggested a new tuned mass damper (TMD) that was designed and optimized using a sequential quadratic programming algorithm. Experiments showed that

the critical depth of the cut had increased as observed from SLD.

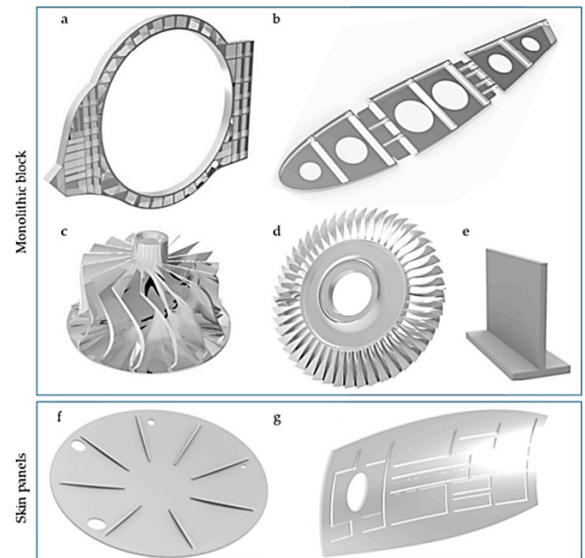


Fig. 1. Typical thin-ribbed aerospace structures; a) frame, b) rib, c) impeller, d) blisk, e) sample part, f) bulkhead, and g) fuselage skin [5]

Fei et al. [6] proposed a moving damper for chatter suppression while milling flexible components

wherein the damper is supported on the back surface of the workpiece. Shui et al. [7] proposed a tuneable stiffness vibration absorber that could be tuned by changing the position of the slider. Sims [8] presented a new analytical solution for tuning methodology and observed that the critical depth of cut improved by 40 % to 50 % compared to using classical TMD. Yang et al. [9] suggested two degrees of freedom (DOF) TMD that has both translational and rotational motions. The proposed method was found to reduce vibration amplitude by 81 % and double the critical depth of cut. Yang et al. [10] proposed a passive damper with tenable stiffness to accommodate variations in part dynamics during thin-wall milling, which reduced the surface roughness by 80 %. Bolsunovsky et al. [11] developed a TMD based on spindle frequency, which had a 20-fold mitigation of vibration amplitude. Wang [12] proposed a new non-linear TMD with a friction-spring element that improved the critical depth of cut by 30 % as compared to the optimally tuned linear TMD.

Yang et al. [13] designed a two-DOF magnetic TMD to mitigate workpiece vibration in multiple modes. Researchers [14] and [15] proposed a passive damping solution using tuned viscoelastic dampers to mitigate the vibration of thin-wall castings focusing on change in coupled interaction between tool and workpiece due to the addition of tuned dampers. Yang et al. [16] investigated numerically the real part-based tuning by employing the minimax numerical approach to maximize the minimum real part of the primary structure under harmonic excitation. They demonstrated the effectiveness by raising the minimum stability limit with single and multiple TMDs. Burtscher and Fleischer [17] proposed an innovative adaptive TMD with variable mass to suppress chatter in the machine tool.

Despite many studies on the application of TMD for chatter suppression, the literature review reveals that no extensive studies on the effect of TMD mounting location on chatter stability of thin-wall workpieces are carried out. Hence, the present work addresses the above gap and focuses on proposing a generalized methodology for optimizing the location of TMD, taking into consideration the mass effect of TMD.

1 METHODOLOGY

In the present work, numerical and experimental methods are used to study the dynamics of a thin-wall workpiece. A TMD is designed based on the modal parameters of the workpiece corresponding to the

dominant mode. A numerical model of the workpiece with TMD is developed to investigate the effect of the location of TMD on chatter stability and optimize the same by using the response surface optimization method.

1.1 Milling Dynamic Model

Precise dynamic modelling of the milling system plays a vital role in the design and analysis of TMDs. In thin-wall milling, the dynamic rigidity of the workpiece rather than the cutter is one of the critical parameters that decide the occurrence of chatter. Moreover, the dynamic rigidity of the workpiece in the normal direction to the cutter axis limits the process stability and material removal rate. Hence, a single degree of freedom milling dynamic model developed by considering only the dynamics of the workpiece to be sufficient to investigate chatter stability in thin wall milling.

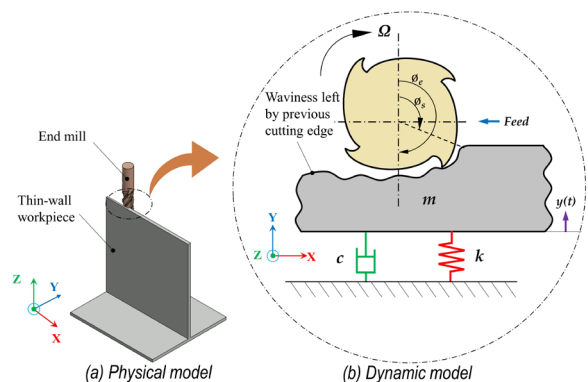


Fig. 2. Single degree of freedom milling dynamic model

A single degree of freedom milling dynamic model proposed by Budak et al. [3], presented in Fig. 2, is adopted for the study. The model consists of a spring-mass-damper system, where m , k , and c respectively represent the modal mass, modal stiffness, and modal damping coefficient at a dominant mode of vibration of the workpiece. The dynamic chip thickness that modulates the cutting force is denoted as $h(t)$. The governing equation of motion of the system shown in Fig. 1 can be written as

$$m\ddot{y} + c\dot{y} + ky = K_s \cdot b \cdot h(t), \quad (1)$$

where, K_s and b are the specific cutting resistance of the workpiece material and axial depth of cut, respectively. According to the regenerative chatter theory, the axial depth of cut at the stability limit of the milling process is given by

$$b_{lim} = \frac{-2\pi}{N_t \alpha_{yy} K_t Re[\Lambda(i\omega_c)]}, \quad (2)$$

where b_{lim} is the limiting depth of cut, N_t is the number of teeth in the cutter, α_{yy} is the directional coefficient in the y -direction K_t is tangential cutting force coefficient, $Re[\Lambda(i\omega_c)]$ is the negative real part of receptance (displacement per unit force) of the workpiece in the y -direction and ω_c is the chatter frequency. The directional dynamic milling coefficient in the y -direction, α_{yy} is given by

$$\alpha_{yy} = \frac{1}{2} [-\cos(2\theta) - 2K_r\theta - K_r \sin(2\theta)]_{\phi_s}^{\phi_e}. \quad (3)$$

In Eq. (3), θ is the tool engagement angle, K_r is the radial milling force coefficient, and ϕ_s and ϕ_e are the start and exit angles of the tool during the machining. The relation between the phase shift (ϵ), the integer number of oscillations (n) between each tooth pass and the chatter frequency (ω_c) can be expressed as

$$\frac{60\omega_c}{\Omega} = 2\pi n + \epsilon, \quad (4)$$

where Ω is the spindle speed of the machine tool. Using Eqs. (2) and (4), the stability lobe diagram can be plotted for different values of n .

1.2 Prediction of Thin-Rib Dynamics

Modal parameters, namely the modal frequency, modal mass, and modal damping ratio corresponding to the dominant mode of the workpiece, play a significant role in the design of TMD for enhanced chatter stability. These parameters are determined with the help of the frequency response function of the workpiece obtained at its critical location. The critical location is the location on the workpiece where the vibration amplitude is maximal. Numerical modal analysis is used to identify the critical location from the mode shapes of the workpiece. A representative thin-wall workpiece (Fig. 3) made of Aluminium 6061 alloy with the following properties is considered for the study: Young’s modulus was 68.9 GPa, Poisson’s ratio 0.33, and density 2700 kg/m³. The bottom face of the base plate is constrained in all directions and the analysis is performed using a commercial finite element code ANSYS Workbench®. A chatter range of 0 Hz to 533 Hz is considered for the analysis, which is the tooth passing frequency range associated with end milling using four flute cutters with a spindle speed range of 0 rpm to 8000 rpm.

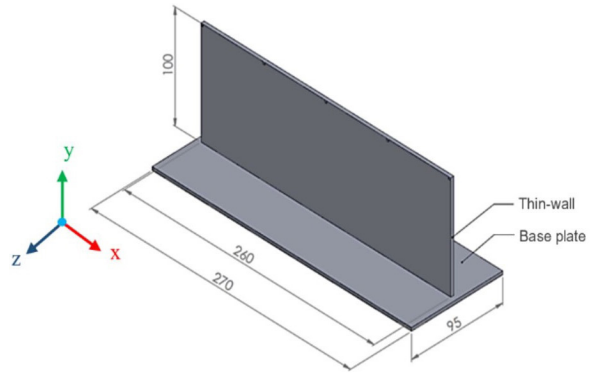


Fig. 3. Thin-walled workpiece

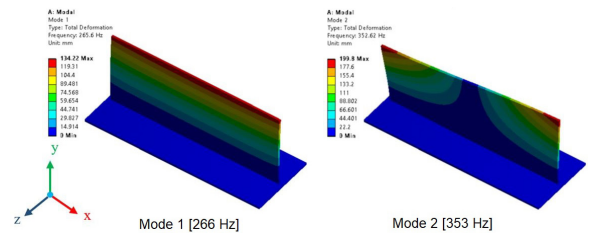


Fig. 4. Mode shapes of workpiece

Fig. 4 depicts the mode shapes of the workpiece obtained from the modal analysis, where the bending mode about the x -axis and twisting mode about the y -axis are observed at 266 Hz and 353 Hz, respectively. The mode shapes are symmetrical to the YZ plane and the locations L1 and L5 (Fig. 5) are identified as critical locations where relative amplitudes of vibration are maximal. Hence, due to the symmetric nature of mode shapes, L1 is considered to be the critical location for subsequent analysis.

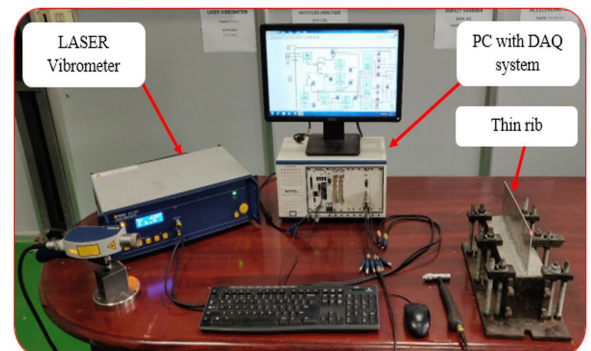


Fig. 5. Experimental setup for impact hammer test

An impact hammer test (Fig. 5) was performed on the workpiece at L1 to determine the dynamic parameters of the workpiece through frequency response function (FRF) measurements. An impact hammer (Make: Brüel & Kjær, sensitivity: 2.097

mV/N) was used to excite the workpiece at L1 with an impulse force of 5 N to 10 N applied in +Y direction and vibration response was recorded right behind L1 using a Laser Doppler Vibrometer (Make: Polytec, model: NLV-2500, sensitivity: 500 $\mu\text{m/V}$). The signals were obtained using a DAQ system (Make: National Instruments, model: PXIe-1078) at a sampling rate of 5 kHz and receptance was estimated using LabVIEW® software.

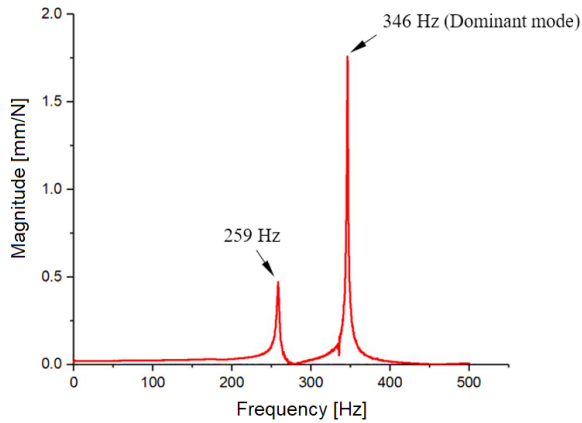


Fig. 6. Magnitude of receptance at location L1

The magnitude of receptance obtained from the test is depicted in Fig. 6, which shows two distinct peaks at 259 Hz and 346 Hz that correspond to the frequencies of 266 Hz and 353 Hz, respectively, as predicted by numerical analysis. A mode at 346 Hz is termed a dominant mode, which has a maximum magnitude of 1.72 mm/N. The damping ratio is identified as 0.0032 for the dominant mode using the half-power bandwidth method. The frequencies obtained by numerical analysis are in close agreement with experimentation with a maximum deviation of 4.2 %, thereby validating the numerical model.

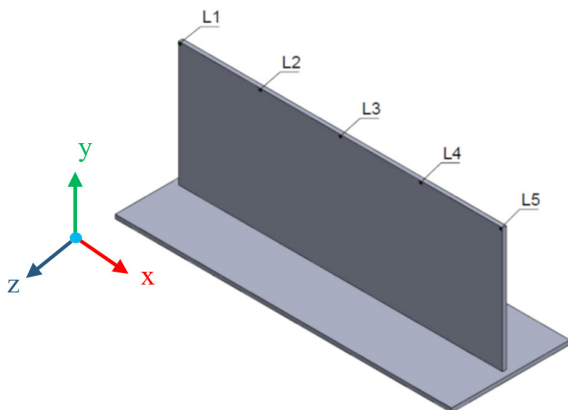


Fig. 7. Excitation locations on the workpiece

The validated model is tuned with the experimentally obtained damping ratio to predict the receptances of the workpiece. It is evident from Eq. (2) that $Re[\Lambda(i\omega_c)]$ of the workpiece is a decisive factor for chatter stability in thin wall milling of a given workpiece material and tool combination. However, $Re[\Lambda(i\omega_c)]$ of the workpiece, in turn, depends on the location of excitation during machining. The harmonic response analysis is performed on the tuned model using ANSYS Workbench® to predict the $Re[\Lambda(i\omega_c)]$ of the workpiece at critical locations. A force of unit magnitude is applied at L1 along the +Y direction, and the frequency of the applied force is swept between 300 Hz to 400 Hz to completely capture the $Re[\Lambda(i\omega_c)]$ of the dominant mode.

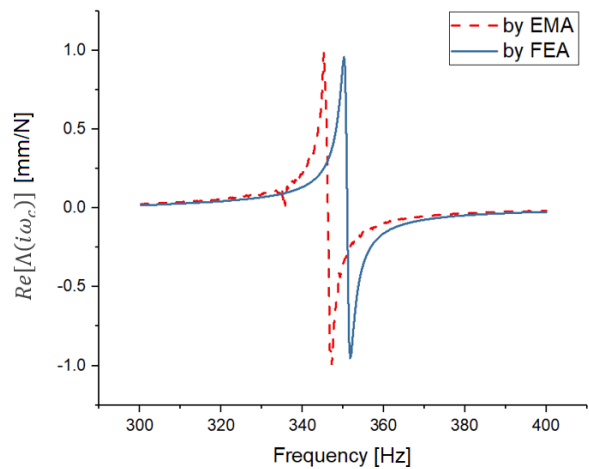


Fig. 8. Comparison of real parts of receptance of L1

A comparison of the real part of receptances of the workpiece at L1 obtained with numerical and experimental methods is shown in Fig. 8. $Re[\Lambda(i\omega_c)]$ predicted using the numerical method is in close agreement with that obtained by experimentation with a frequency shift of 7 Hz corresponding to a 2 % deviation in natural frequency. Furthermore, $Re[\Lambda(i\omega_c)]$ obtained with the numerical method is -0.9525 mm/N, which is in close agreement with the experimental result of -0.9902 mm/N with a maximum deviation of 4 %.

1.3 Design of Tuned Mass Damper (TMD)

The modal stiffness (k) of the workpiece is calculated from the negative maximum of the imaginary part of receptance $Im[\Lambda(i\omega_c)]$ and damping ratio measured at L1 by the Eq. (5) [18].

$$k = \frac{-1}{2\zeta \min(Im[\Lambda(i\omega_c)])}. \quad (5)$$

The modal stiffness of the workpiece corresponding to $Im[\Lambda(i\omega_c)]$ of -1.71 mm/N is calculated as 127.13 kN/m and the modal mass is found to be 0.0269 kg . A mass ratio (μ) of 5% [8] is used to design the TMD. The stiffness of the TMD is computed using Eq. (6) [18].

$$\frac{f_r}{f_w} = \sqrt{\frac{\mu + 2 + \sqrt{2\mu + \mu^2}}{2(1 + \mu)^2}}, \quad (6)$$

where, f_r , f_d and f_w are the frequency ratio, the natural frequency of the damper and the dominant frequency of the workpiece, respectively. The design parameters of TMD are calculated and are presented in Table 1.

Table 1. Design parameters of TMD

| | |
|------------------------|--------|
| Frequency ratio | 1.036 |
| Natural frequency [Hz] | 358 |
| Effective mass [kg] | 0.0013 |
| Stiffness [kN/m] | 6.58 |

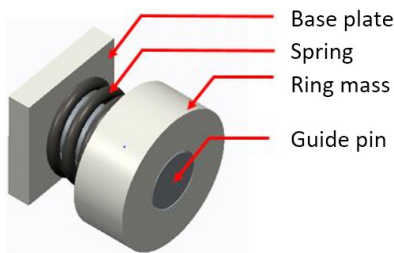


Fig. 9. Proposed design of TMD

Fig. 9 shows a proposed design of TMD, which consists of a ring mass, guide pin, base plate, and a helical compression spring. The base plate of the TMD is made of an aluminium sheet of 3 mm thickness. Steel dowel pins of 2.5 mm and 25 mm long are used as guide pins. An open coil helical spring of mean coil diameter, wire diameter, free length, and number of active coils of 10 mm , 1 mm , 10 mm , and 3 turns, respectively, is designed to obtain the required stiffness.

1.4 Effect of Location of TMD on Chatter Stability

Some of the applications of TMD based on conventional approaches may not yield optimum performance in thin wall milling. Therefore, the location on the workpiece that results in an optimum

mass ratio needs to be identified by considering the stationary component of TMD.

A TMD having a single degree of freedom is designed based on the design parameters obtained in the previous section. The TMD is mounted on one of the locations on the workpiece defined by X and Y coordinates about the coordinate system, as shown in Fig. 10. A COMBIN14 element with longitudinal stiffness of 6.58 kN/m is used between the ring mass and the base plate of the TMD. A frictionless contact is applied between the ring mass and the guide pin, and the base plate of the TMD is attached to the workpiece using a bonded connection.

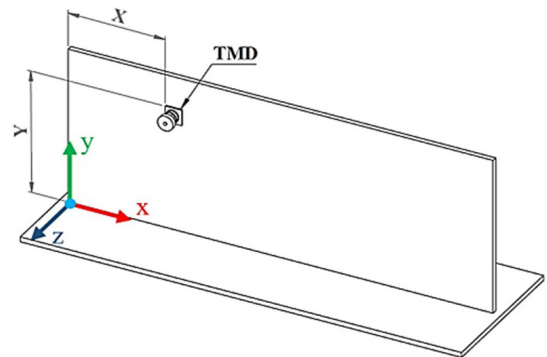


Fig. 10. TMD and its location on the workpiece

Parameterized harmonic response analysis was carried out with coordinates of damper location (X, Y) as input parameters and the magnitude of the negative maximum of imaginary parts of receptance ($Im[\Lambda(i\omega_c)]$) as an output parameter. Thirty-six mounting locations of TMD on the workpiece were considered for the investigation.

Custom design of experiments with 36 design points as the coordinate of the damper is employed for the analysis. The X-coordinate of the damper is varied from 0 mm to 260 mm in steps of 65 mm along the length of the plate. Similarly, the Y-coordinate of the damper is varied from 25 mm to 100 mm in steps of 25 mm . Harmonic response analysis is performed on the workpiece for location L1 and the negative maximum of the real part of receptance of the ($Re[\Lambda(i\omega_c)]$) is noted for all the thirty-six locations of TMD.

Similar analyses are carried out for the other two excitation locations L2 and L3 and the results presented as response surfaces as shown in Fig. 11, which portrays the effect of TMD location on the negative ($Re[\Lambda(i\omega_c)]$) of the workpiece three excitation locations.

Since the workpiece is geometrically symmetrical about the YZ plane, which passes through L3, the

contours of $|\text{Re}[\Lambda(i\omega_c)]|$ of L5 and L4 will be the mirror images of the contours of that of L1 and L2, respectively. As L3 is the node point for mode 2, it exhibits the least value for $|\text{Re}[\Lambda(i\omega_c)]|$ in almost all the locations of the damper except for L1 and L5.

excitation. Hence, the optimum location of TMD needs to be identified for effective chatter suppression.

1.5 Optimization of TMD Location for Enhanced Chatter Stability

The optimum location of the damper for enhancing the chatter stability of the workpiece is carried out by employing response surface optimization. The response surfaces obtained for are optimized using genetic algorithms. The basic flow chart for carrying out parameterized harmonic analysis followed by optimization is shown in Fig. 12. The optimization is performed for each of the five excitation locations to minimize the of the workpiece. Three candidate points that represent the optimal locations for the damper on the workpiece are obtained for each excitation location.

It is inferred from Table 2 that the Y-coordinates for the candidate points of all excitation locations remain the same irrespective of X-coordinates. The average Y-coordinate of damper for minimizing is found to be 98.6 mm, which is 98 % of the height of the part from the base. The corresponding to the critical location L1 is found to be higher in comparison to other locations as expected. Considering the critical locations L1 and L5, it is evident from Table 2 that the coordinates, as well as the objective equation values, are quite close to each other for all the three candidate points. Therefore, the average X-coordinate of the damper for minimizing chatter is found to be 65 mm, which is at 25 % of the length of the workpiece from the respective excitation locations. Hence, the TMD is placed on the workpiece at $(X, Y) = (65, 99)$ mm and harmonic response analysis is performed for each of the excitation locations of the workpiece.

Table 2. Optimal locations of damper for each excitation location

| Location | Candidate point | Coordinates [mm] | | Objective equation values |
|----------|-----------------|------------------|-------|--|
| | | X | Y | Max $(\text{Re}[\Lambda(i\omega_c)])$ [mm/N] |
| L1 | 1 | 65.89 | 98.79 | -0.4691 |
| | 2 | 63.89 | 98.45 | -0.4692 |
| | 3 | 61.77 | 98.83 | -0.4688 |
| L2 | 1 | 47.30 | 98.81 | -0.1942 |
| | 2 | 51.33 | 98.95 | -0.1924 |
| | 3 | 53.70 | 98.77 | -0.1908 |
| L3 | 1 | 62.48 | 98.63 | -0.0107 |
| | 2 | 195.62 | 98.69 | -0.0106 |
| | 3 | 76.62 | 96.22 | -0.0089 |

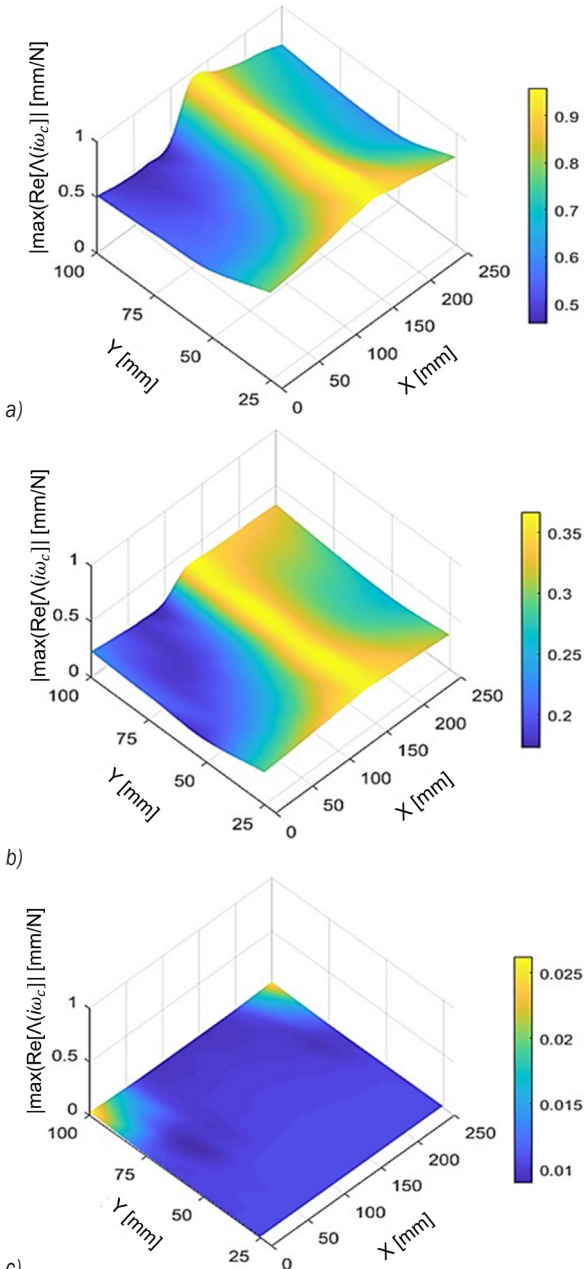


Fig. 11. Effect of TMD location a) L1, b) L2 and c) L3 on $(\text{Re}[\Lambda(i\omega_c)])$

It is inferred from Fig. 11 that the damper is ineffective for all values of Y when it is located at $X = 130$ mm and most effective near the location of

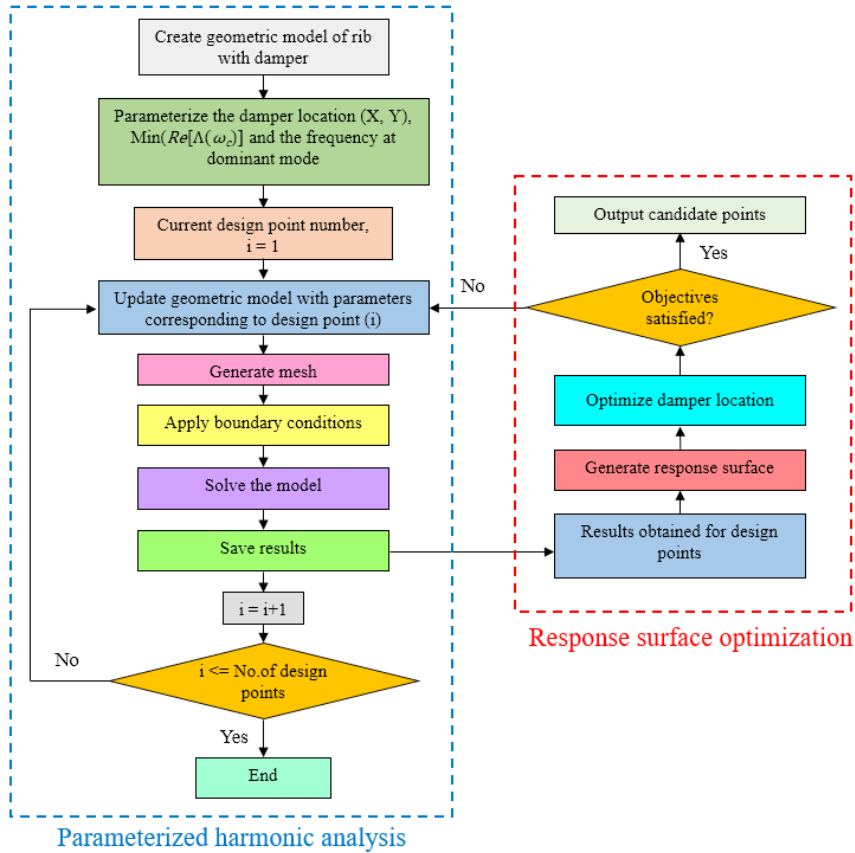


Fig. 12. Flow chart for parameterized harmonic analysis and optimization

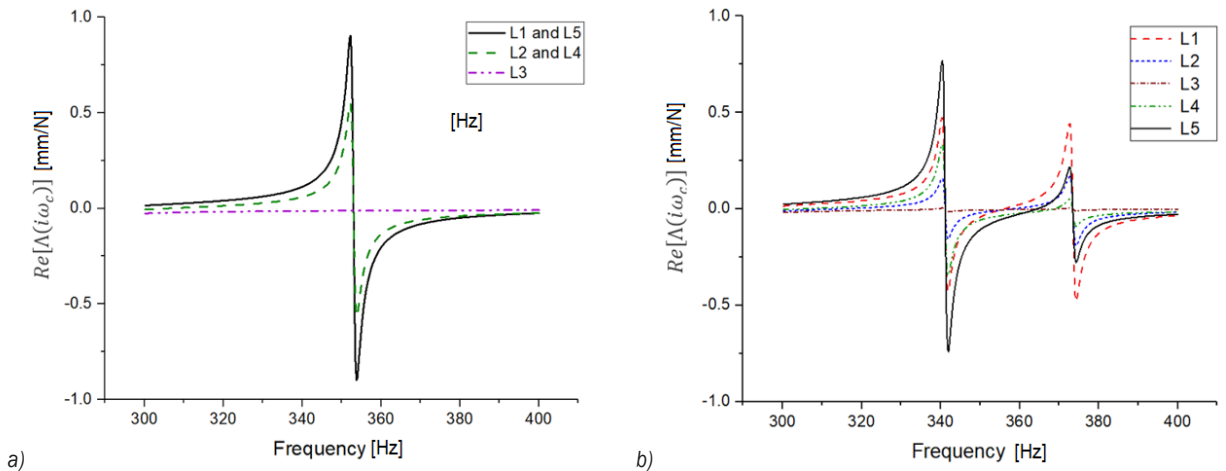


Fig. 13. Comparison of $Re[\Lambda(i\omega_c)]$ a) with and b) without TMDs

A comparison of the real parts of receptance of the plate with and without TMD is shown in Fig. 13. It is inferred from Fig. 13 that negative ($Re[\Lambda(i\omega_c)]$) of the workpiece at L1 is reduced from -0.9542 mm/N to -0.4687 mm/N, which corresponds to about a 51 % improvement in dynamic stability. Also, the TMD is

found to be effective for the locations L1, L2, and L3 and least effective for L4 and L5 when located at the optimum location for L1. This implies that the use of a single TMD is effective when the cutter traverses between L1 and L3 and is least effective between L3 and L5. Therefore, one more TMD with the same

modal parameters was designed and located at the optimum location for L5 and the harmonic response analyses were repeated for L1 and L5.

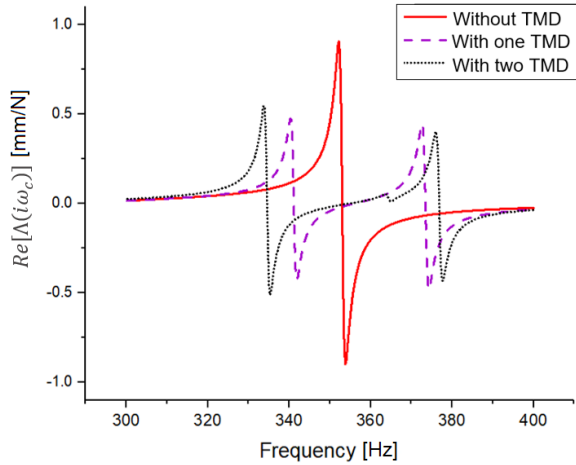


Fig. 14. Real parts of receptance at L1 and L5

Fig. 14 depicts the comparison of the real part of receptance obtained at L1 and L5 of the workpiece without TMD, with one TMD and two TMDs. It is evident from the figure that the use of two TMDs considerably minimizes $Re[\Lambda(i\omega_c)]$ at L5 from 0.7417 mm/N to 0.511 mm/N, which correspond to an improvement of 31 % when compared to the use of one TMD and 46 % without TMD. Even though the negative maximum values of Re of the workpiece at L1 and L5 are minimized using two TMDs, there is a drop in the corresponding chatter frequencies from 353 Hz to 336 Hz.

2 EXPERIMENTAL VALIDATION OF OPTIMUM LOCATION OF TMD

2.1 Impact Hammer Test on Workpiece with TMDs

TMDs were fabricated as per the design parameters obtained in the previous section. Ring masses are prepared by stacking and gluing the brass washers of outer diameter, inner diameter and thickness of 16 mm, 5 mm, and 0.3 mm, respectively. Each washer weighs about 4.75 g, and three washers are used to achieve a total mass of 2.75 g, which is slightly larger than the required mass of 2.69 g. The increased mass of the ring mass alters the mass ratio from 5 % to 5.2 %, which is negligible and insignificant. The prepared TMDs were mounted on the workpiece at optimum locations obtained in the previous section. Fig. 15 shows the workpiece with TMDs in which TMD1 and TMD2 were mounted at the optimum locations

corresponding to L1 and L5, respectively. Initially, the impact hammer test was carried out with one TMD mounted at an optimum location and then with both the TMDs mounted at their optimum locations.

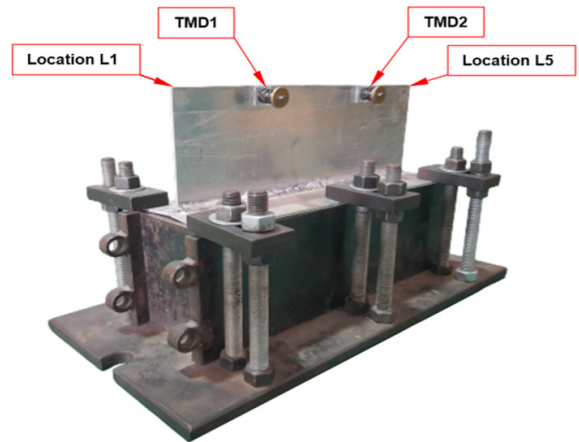


Fig. 15. Thin-walled workpiece with TMDs

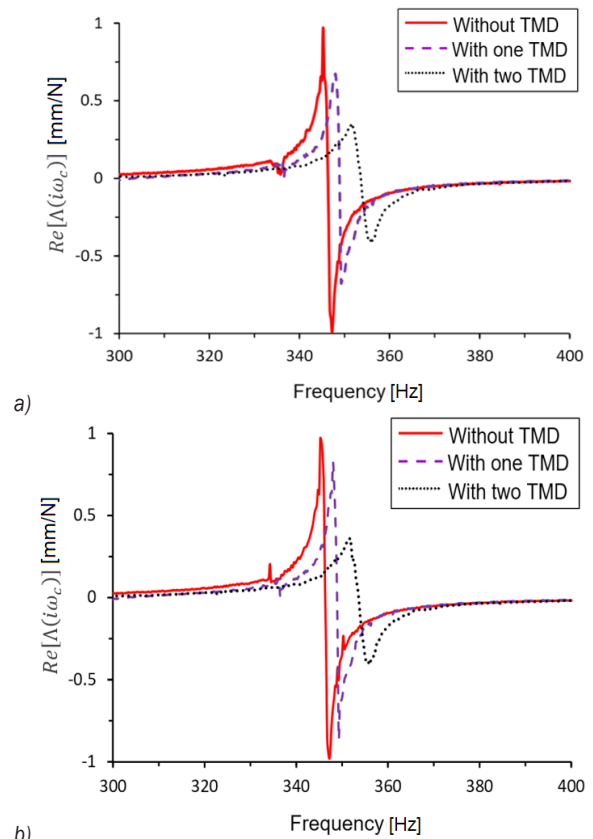


Fig. 16. Comparison of real part of receptances; a) location L1, and b) location L5

The comparison of Re obtained at critical locations L1 and L5 are shown in Figs. 16a and b, respectively. It is inferred from Figs. 16a and b that

the negative real parts of receptance of the workpiece are minimized at both critical locations of the workpiece after the introduction of TMDs. When one TMD is located at the optimum location for L1, there is a marginal improvement in negative Re of L5 as observed as predicted by numerical analysis.

The marginal improvement in Re of L5 is attributed to the inertial effect of TMD located at L1. It is also revealed from Fig. 16b that a considerable improvement in the dynamic stability of the workpiece is observed on applying two TMDs at their optimum locations.

The Re of the workpiece at critical locations for the cases without TMD, with one TMD and with two TMDs are found to be about -0.9902 mm/N, -0.6747 mm/N, and -0.3952 mm/N, respectively, which correspond to 32 % and 60 % improvements in the dynamic stability of the workpiece.

2.2 Machining Test

The chatter stability of the undamped and damped workpiece was predicted and compared by using SLDs which were plotted (Fig. 17) by using the modal parameters and the identified cutting coefficients of the workpiece material, namely $K_{tc} = 792.8$ N/mm², $K_{rc} = 157.5$ N/mm², $K_{ac} = 208.0$ N/mm², $K_{te} = 22.9$ N/mm, $K_{re} = 25.6$ N/mm, and $K_{ae} = 1.6$ N/mm. A comparison of SLDs of the workpiece without TMD and that with two TMDs is depicted in Fig. 17. It is observed that the minimum stable depths of cut of the undamped and damped workpiece are in the order of 0.08 mm and 0.24 mm, respectively, which correspond to a three-fold improvement in the chatter stability of the workpiece.

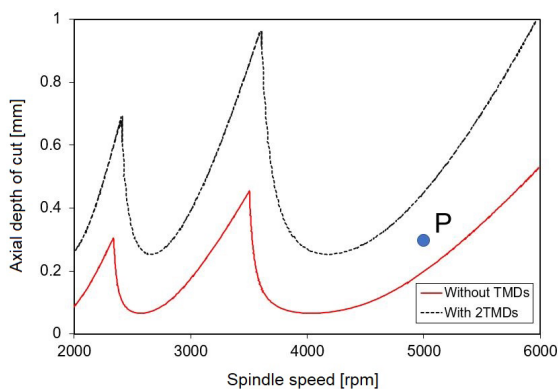


Fig. 17. Stability lobe diagrams

The application of TMDs for rough milling may not be feasible as a large amount of material needs to be removed from both sides of the workpiece which

hinders machining operation and greatly alters the structural dynamics. Also, the surface roughness is of least consideration in rough milling. However, chatter needs to be avoided during finish milling as it affects the surface quality of the machined part. The chatter stability during finish milling of thin walls can be improved by mounting the TMDs on a surface that is opposite to the surface of the thin wall being machined.

Milling tests were carried out on a three-axis machining centre (Jyoti & Model: RDX20) shown in Fig. 18, using a carbide milling cutter of diameter 16 mm with 4 flutes. The TMDs were mounted at their optimum locations on the surface of the thin wall just behind the surface being machined. Down milling was carried out on the damped and undamped parts on the part surface opposite to the surface where TMDs were placed. The test was conducted under similar cutting conditions to validate the damping characteristics of TMDs. Similar cutting parameters, namely a feed rate of 1200 m/min, spindle speed of 5000 rpm, axial depth of cut of 0.3 mm and radial depth of cut of 1 mm were selected from the SLDs. The above parameters were selected so that point P (Fig. 17) lies in the region of the SLD which results in unstable machining without TMDs. A uniaxial accelerometer (Dytran 3224A1 with a sensitivity of 9.68 mV/g) was used to acquire vibration signals during milling. The time domain and frequency domain signals, along with the machined surface quality, with and without TMDs are shown in Fig. 19.

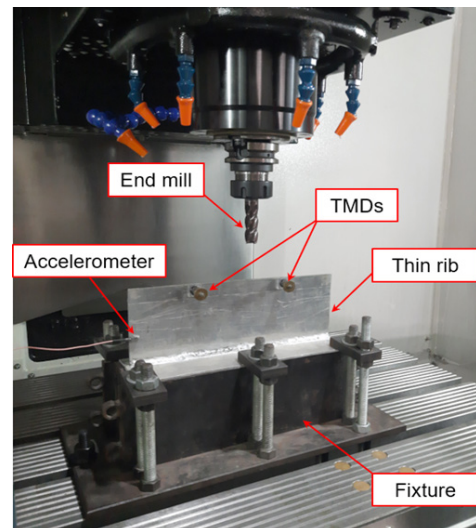


Fig. 18. Experimental setup for machining tests

It is observed from the figure that the magnitude of vibration has reduced from 38 g to 18 g after

3 CONCLUSIONS

introducing TMDs. It can also be observed from the frequency spectrum that the spike at 340 Hz (chatter frequency of undamped workpiece) has vanished. Because of the above, the damped workpiece does not exhibit chatter marks, as shown in Fig. 19b. The setup for surface roughness measurement is shown in Fig. 20. The surface roughness of the machined workpieces was measured using a surface roughness tester (Make: Kosaka Lab, Model: SE-1200) with a diamond stylus of 5 μm radius at a measuring speed of 0.2 m/s.

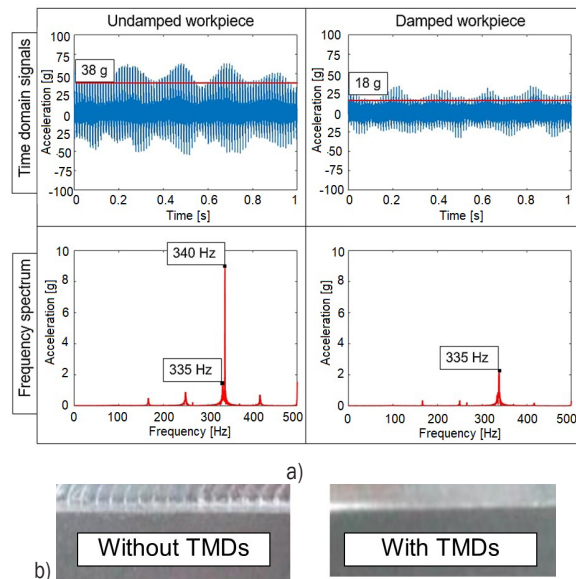


Fig. 19. Results of experimentation; a) vibration signals obtained during milling tests, and b) surface quality of the machined parts

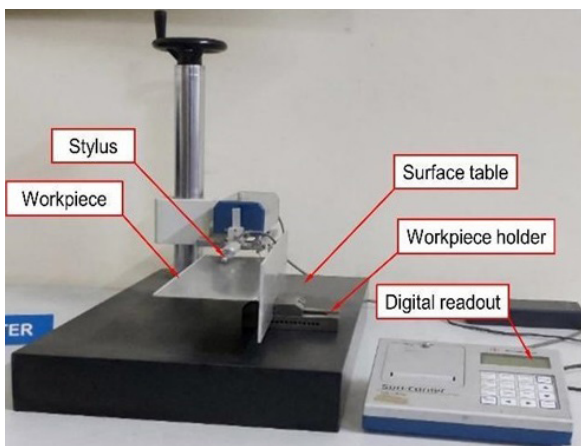


Fig. 20. Setup for surface roughness measurement

The average surface roughness (R_a) of the undamped and damped workpieces are found to be 4.24 μm and 2.63 μm , respectively, which correspond to an improvement in surface finish by 38 %.

A novel methodology for optimizing the TMD location towards enhancing chatter suppression in thin-wall milling considering the mass effect of TMDs is presented. The optimization of TMD location is carried out based on a parameterized harmonic analysis aided with a response surface methodology. The effectiveness of the proposed methodology is assessed by plotting SLDs followed by a series of milling tests. The results reveal that chatter in thin-wall milling can be suppressed to a great extent with the proposed approach. The following are the major conclusions drawn from the research work:

- The location of TMD is a crucial factor that influences the dynamic stability of the workpiece at critical mode.
- The optimal X- and Y-coordinates of TMD location for effective chatter suppression of the thin-walled workpiece with dominant mode as torsional mode are about 25 % of the length from either end, and 99 % of the height of the workpiece, respectively.
- Use of a single TMD is found to be effective only for the first half of the cutter path whereas two TMDs are required to improve chatter stability while machining along the entire path.
- Milling tests revealed that the application of TMDs yielded a 60 % improvement in the overall dynamic stability of the workpiece which corresponds to a three-fold improvement in productivity with an enhanced surface finish of 38 %.

The above results portray the effectiveness of the proposed method. Even though the method is validated using a simple thin-walled part, it can also be applied to improve the chatter stability of complex thin-wall structures, such as turbine blades, impellers, and other aircraft and automobile parts, where one just needs to design and locate TMDs at their optimum locations.

4 NOMENCLATURES

- m modal mass, [kg]
- c modal damping coefficient, [Ns/m]
- k modal stiffness, [kN/m]
- ζ modal damping ratio, [-]
- f_r frequency ratio, [-]
- f_d frequency of TMD, [Hz]
- f_w frequency of workpiece, [Hz]
- Λ frequency response function, [mm/N]
- ω_c chatter frequency, [rad/s]

K_{tc} tangential cutting force coefficient, [N/mm²]
 K_{rc} radial cutting force coefficient, [N/mm²]
 K_{ac} axial cutting force coefficient, [N/mm²]
 K_{te} tangential edge force coefficient, [N/mm²]
 K_{re} radial edge force coefficient, [N/mm²]
 K_{ae} axial edge force coefficient, [N/mm²]

5 ACKNOWLEDGEMENTS

The authors would like to express their sincere thanks to the management of PSG College of Technology, Coimbatore and the Office of Principal Scientific Advisor to GoI, New Delhi for providing the necessary facilities for carrying out this research work.

6 REFERENCES

- [1] Altintas, Y., Budak, E. (1995). Analytical prediction of stability lobes in milling. *CIRP Annals*, vol. 44, no. 1, p. 357-362, DOI:10.1016/S0007-8506(07)62342-7.
- [2] Budak, E., Tunç, L.T., Alan, S., Özgüven, H.N. (2012). Prediction of workpiece dynamics and its effects on chatter stability in milling. *CIRP Annals*, vol. 61, no. 1, p. 339-342, DOI:10.1016/j.cirp.2012.03.144.
- [3] Iglesias, A., Munoa, J., Ciurana, J., Dombóvári, Z., Stépán, G. (2016). Analytical expressions for chatter analysis in milling operations with one dominant mode. *Journal of Sound and Vibration*, vol. 375, p. 403-421, DOI:10.1016/j.jsv.2016.04.015.
- [4] Yuan, H., Wan, M., Yang, Y., (2019). Design of a tunable mass damper for mitigating vibrations in milling of cylindrical parts. *Chinese Journal of Aeronautics*, vol. 32, no. 3, p. 748-758, DOI:10.1016/j.cja.2018.12.002.
- [5] Del Sol, I., Rivero, A., López de Lacalle, L.N., Gamez, A.J. (2019). Thin-wall machining of light alloys: A review of models and industrial approaches. *Materials*, vol. 12, no. 12, art. ID 2012, DOI:10.3390/ma12122012.
- [6] Fei, J., Lin, B., Yan, S., Ding, M., Xiao, J., Zhang, J., Zhang, X., Ji, C., Sui, T. (2017). Chatter mitigation using moving damper. *Journal of Sound and Vibration*, vol. 410, p. 49-63, DOI:10.1016/j.jsv.2017.08.033.
- [7] Shui, X., Wang, S. (2018). Investigation on a mechanical vibration absorber with tunable piecewise-linear stiffness. *Mechanical Systems and Signal Processing*, vol. 100, p. 330-343, DOI:10.1016/j.ymssp.2017.05.046.
- [8] Sims, N.D. (2007). Vibration absorbers for chatter suppression: a new analytical tuning methodology. *Journal of Sound and Vibration*, vol. 301, no. 3-5, p. 592-607, DOI:10.1016/j.jsv.2006.10.020.
- [9] Yang, Y., Muñoa, J., Altintas, Y. (2010). Optimization of multiple tuned mass dampers to suppress machine tool chatter. *International Journal of Machine Tools and Manufacture*, vol. 50, no. 9, p. 834-842, DOI:10.1016/j.ijmactools.2010.04.011.
- [10] Yang, Y., Xie, R., Liu, Q. (2017). Design of a passive damper with tunable stiffness and its application in thin-walled part milling. *The International Journal of Advanced Manufacturing Technology*, vol. 89, p. 2713-2720, DOI:10.1007/s00170-016-9474-7.
- [11] Bolsunovsky, S., Vermel, V., Gubanov, G., Leontiev, A. (2013). Reduction of flexible workpiece vibrations with dynamic support realized as tuned mass damper. *Procedia CIRP*, vol. 8, p. 230-234, DOI:10.1016/j.procir.2013.06.094.
- [12] Wang, M. (2011). Feasibility study of nonlinear tuned mass damper for machining chatter suppression. *Journal of Sound and Vibration*, vol. 330, no. 9, p. 1917-1930, DOI:10.1016/j.jsv.2010.10.043.
- [13] Yang, Y., Dai, W., Liu, Q. (2017). Design and machining application of a two-DOF magnetic tuned mass damper. *The International Journal of Advanced Manufacturing Technology*, vol. 89, p. 1635-1643, DOI:10.1007/s00170-016-9176-1.
- [14] Zhang, Z., Li, H., Liu, X., Zhang, W., Meng, G. (2018). Chatter mitigation for the milling of thin-walled workpiece. *International Journal of Mechanical Sciences*, vol. 138-139, p. 262-271, DOI:10.1016/j.ijmecsci.2018.02.014.
- [15] Kolluru, K.V., Axinte, D.A., Raffles, M.H., Becker, A.A. (2014). Vibration suppression and coupled interaction study in milling of thin wall casings in the presence of tuned mass dampers. *Proceedings of the Institution of Mechanical Engineers, Part B: Journal of Engineering Manufacture*, vol. 228, no. 6, p. 826-836, DOI:10.1177/0954405413508769.
- [16] Yang, Y.Q., Chen, T.T. (2012). Numerical solution of tuned mass dampers for optimum milling chatter suppression. *Materials Science Forum*, vol. 697-698, p. 223-228, DOI:10.4028/www.scientific.net/MSF.697-698.223.
- [17] Burtscher, J., Fleischer, J. (2017). Adaptive tuned mass damper with variable mass for chatter avoidance. *CIRP Annals*, vol. 66, no. 1, p. 397-400, DOI:10.1016/j.cirp.2017.04.059.
- [18] Schmitz, T.L., Smith, K.S. (2014). *Machining Dynamics*. Springer, New York, DOI:10.1007/978-0-387-09645-2.